Symposium on Compact Heat Exchangers,
A Festschrift on the 60th Birthday of Ramesh K. Shah,
24 August 2002, Grenoble, France, pp.401~406

Forced Convective Boiling Heat Transfer in Microtubes at Low Mass and Heat Fluxes

Tzu-Hsiang Yen, Nobuhide Kasagi and Yuji Suzuki
Department of Mechanical Engineering, The University of Tokyo, Bunkyo-ku, Hongo 7-3-1, Tokyo

The convective boiling in micro tubes of 0.19, 0.3 and 0.51mm ID was investigated with relatively small wall heat fluxes and mass flow rates. In this experiment, we have found some peculiar superheat phenomenon, which deteriorates the heat transfer coefficient. The region of the onset of superheat is plotted in the flow map. The heat transfer coefficient distributions in the saturated boiling region without superheat are measured and found different from those in traditional and small-size tubes. The associated pressure loss becomes larger as the inner diameter is decreased in accordance with the existing empirical correlations.

Nomenclature

Bo: boiling number, $Bo=q''/h_{lv}G$
C_p: specific heat [J/kg K]
f: friction factor
D_o: outer tube diameter [m]
D_i: inner tube diameter [m]
$\dot{m}$: mass flux [kg/m^2 s]
h_{loss}: heat loss coefficient [W/m^2 K]
h_{lv}: latent heat [J/kg]
h_{sat}: saturated boiling heat transfer coefficient [W/m^2 K]
I: electric current through the test section [A]
l: subcooled length [m]
L: total test section length [m]
$\dot{M}$: mass flow rate [kg/s]
P_{avg}: test section average pressure [kPa]
P_{in}: test section inlet pressure [Pa]
P_{out}: test section outlet pressure [Pa]
P_{sat}: pressure when the subcooled liquid reaches the saturated temperature [Pa]
ΔP_{sub}: Pressure loss of the subcooled region [Pa]
ΔP_{sup}: Pressure loss of the superheated region [Pa]
ΔP_{total}: Total pressure loss of the test section [Pa]
q'': Heat flux [W/m^2]
q''_{loss}: Heat loss [W/m^2]
R: electric resistance [Ω]
r: radial coordinate
s: axial position in the saturated region
T_{air}: environment temperature [^{o}C]
T_{ref}: refrigerant temperature [^{o}C]
T_{wout}: outer wall temperature [^{o}C]
T_{win}: inner wall temperature [^{o}C]
x: axial coordinate [m]
χ: vapor quality

1. Introduction

Micro heatpipes or microchannels are regarded as promising heat exchange devices in modern miniaturized applications such as electronic equipment cooling. In the last decade, intensive research effort was made in this field [1], [2]. Compared to convective boiling in tubes of traditional (> 3 mm) or small size (0.6 mm~ 3 mm, according to the definition by Kandlikar [2]), the heat transfer characteristics are much different with peculiar liquid superheat phenomena discovered [3].

Paitoonsurikarn et al. [4] proposed a new optimal design method for the compact heat exchangers of micro bare tubes without conventional extended surfaces. The efficiency is drastically improved over commercial louver-finned heat exchangers. In their optimal design procedure, however, they use empirical correlations of convective boiling in larger tubes (> 2 mm) for estimating the heat transfer coefficient and the pressure loss in smaller diameter tubes. Moreover, they do not take into account the onset of liquid superheat phenomena. The above treatments may introduce large error in the optimal design.

Convective boiling experiments in traditional tubes have been carried out over several decades. According to these results, the heat transfer coefficient is known to be mainly affected by vapor quality, mass flux, heat flux, tube inner diameter and working fluid. Recently, the convective boiling experiments in tubes of smaller ID from 1.95 to 4 mm were carried out [5]. Unlike the results in traditional-size tubes, the heat transfer coefficient is very weakly dependent on mass flux and vapor quality.

Until now, the convective boiling heat transfer in microtubes of inner diameter less than 1mm still remains unclear. Little research work is available, except Ravigururajan [6]. In his research, the heat transfer coefficient decreases with increasing the vapor quality and the wall superheat. Since these phenomena are completely different from those observed in traditional tubes, they need to be further examined.

In view of a lack of knowledge on optimal design method of micro bare-tube evaporators and for observing the unusual heat transfer and pressure loss characteristics in microtubes, the present work is undertaken with the objectives: (1) to clarify the parameters responsible for the onset of liquid superheat, which deteriorates the heat transfer, and (2) to investigate the heat transfer and pressure loss of convective boiling in microtubes. To do this, we carried out a series of experiments on saturated convective boiling in microtubes of 0.19, 0.3 and 0.51 mm ID at low heat (1~13 kW/m^2) and mass (50~300 kg/m^{2}s) fluxes.

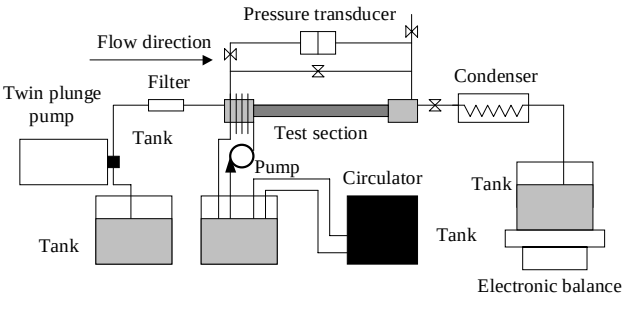

Fig. 1 Experimental loop.

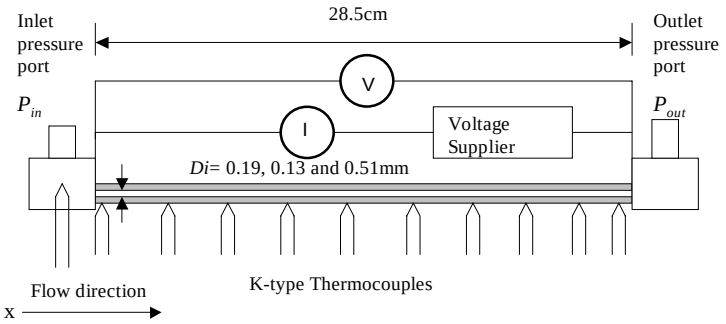

Fig. 2 Test section.

2. Experimental apparatus and procedure

The experimental loop is shown in Figure 1. HCFC123 and FC72 were employed as working fluids. A twin plunge pump (Moleh, MT-2221) was employed to provide constant mass fluxes from 50 to 300 kg/m²s in most of the experiments carried out. Unlike a single plunge pump, the twin plunge pump can provide a stable volume flow rate and minimize unwanted bubbles in the working fluid. The uncertainty of the flow rate is within +2%. The inlet fluid temperature was kept constant in the inlet manifold with a secondary water loop and at 10 ^{O}C below the saturated temperature. The mass flux was determined by the volume flow rate of the pump.

Figure 2 shows the test section of 28+0.5 cm in length. Three different SUS304 stainless steel tubes, having inner/outer diameters of 0.19/0.41, 0.3/0.55, 0.51/0.81 mm, respectively, were employed as a test section. Twelve K-type thermocouples of 25 μm OD were glued onto the outer tube wall with highly conductive silicon. One K-type thermocouple was inserted into the inlet manifold in order to measure the inlet fluid temperature. Cold junctions of the thermocouples were submerged into an icebox. All thermocouples were calibrated with an accuracy of +0.1 K.

In the case of 0.3 mm ID tube experiment, however, we employed a syringe pump and thermocouples with an accuracy of +0.2 K. Periodic flow (duration 150~600 s) driven by the syringe pump made the heat transfer somewhat unstable in the experiments. Thus, we will use these data complementarily in this paper.

The pressure loss was measured by a diaphragm pressure transducer through pressure ports at the inlet and outlet of the test section. The accuracy of the pressure transducer is within +0.1kPa.

In order to examine the accuracy of the pressure measurement and the tube diameter, a single-phase flow experiment was carried out. As shown in Fig. 3, the friction factors measured are in good agreement with the theoretical relation for laminar Poiseuille flows.

The test section was heated by a DC current and covered with glass cotton to reduce the heat loss to the environment. The heat loss was compensated with the procedure described later.

We define a steady state in such a way that the pressure variation falls below +0.1kPa in the case of 0.19mm ID and +0.5kPa in the case of 0.51mm ID, respectively. It usually takes one hour to reach this state during each run.

3. Data reduction

The heat transferred to the fluid q'' is calculated as:

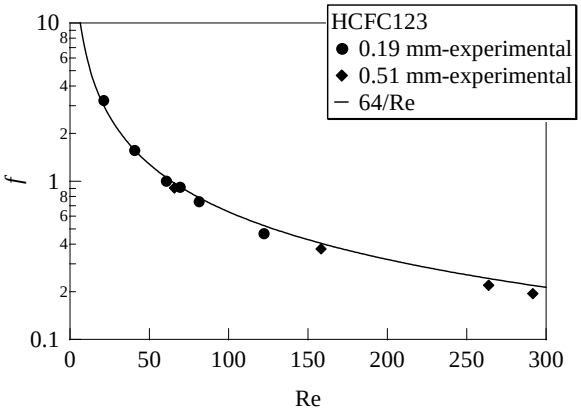

Fig. 3 Friction factor in single phase laminar flow.

$$q'' = I^2R/\pi D_i L - q''_{loss}. \tag{1}$$

The heat loss to the environment q''_{loss} is assumed to be as a function of the wall temperature T_{wout} and the environmental temperature T_{air},

$$q''_{loss} = h_{loss}\left(T_{wout} - T_{air}\right), \tag{2}$$

where h_{loss} is determined by a preliminary heat transfer experiment without the working fluid inside the tube.

The inner wall temperature T_{win} is calculated by solving the one-dimensional heat conduction equation with the boundary conditions,

$$-k\left(\frac{\partial T}{\partial r}\right)_{r=D_O/2} = q''_{loss}, \tag{3}$$

$$T = T_{wout}, \tag{4}$$

at the outer surface of the tube. After onset of the saturated boiling, the working fluid temperature, T_{ref} is assumed to be at the saturated temperature, which depends on the local pressure variation described later. The heat transfer coefficient is then calculated as:

$$h_{sat} = \frac{q''}{T_{win} - T_{ref}}. \tag{5}$$

Since the fluid is heated from subcooled liquid to superheated vapor in the test section, the total pressure loss ΔP_{total} can be written as:

$$\Delta P_{total} = \Delta P_{sub} + \Delta P_{sat} + \Delta P_{sup}, \quad (6)$$

where ΔP_{sub}, ΔP_{sat}, and ΔP_{sup} are the pressure losses in the subcooled liquid, saturated boiling, and superheated vapor regions, respectively. The length of the subcooled region l and the pressure loss are determined by solving iteratively the following equations:

$$\Delta P_{sub} = f \frac{1}{2} \rho U^2 \frac{l}{d}, \quad (7)$$

$$P_{in} - \Delta P_{sub} = P_{sat}, \quad (8)$$

$$\int_0^l \left(\frac{I^2 R}{L} - h_{loss}(x)\left(T_w(x) - T_{air}\right)\pi D_o \right) dx = \dot{M} C_p \left(T_{sat} - T_{in}\right), \quad (9)$$

Equation (7) is the laminar flow pressure loss, while Eq. (9) represents the energy balance. The saturated temperature T_{sat} is determined by a known relationship between T_{sat} and P_{sat}.

The average vapor quality χ in the saturated region is calculated from the balance of heat transfer and the latent heat as:

$$\chi = \frac{\int_l^{l+s} \left(\frac{I^2 R}{L} - h_{loss}(x)\left(T_{wout}(x) - T_{air}\right)\pi D_o \right) dx}{\dot{M} h_{lv}}. \quad (10)$$

The length of the saturated region s is determined from the above integration in such a way that $\chi = 1$.

The pressure loss ΔP_{sup} in the superheat region ($s+l < x < L$) is determined by the laminar flow solution, where the physical properties are determined by the iterative calculation of pressure loss and temperature distribution. The local pressure P_{local} is assumed to be linearly distributed in the saturated boiling region, and given by

$$P_{local} = P_{sat} - \left[P_{sat} - \left(P_{out} + \Delta P_{sup} \right) \right] \frac{x - l}{s} \quad (11)$$

4. Experimental results

4.1 Wall temperature

When the pressure loss of the test section reaches the steady state described in Chapter 2, the wall temperature shows some time history, i.e. sine-wave-like temperature variation of a 20 seconds period and the amplitude of 0.3K in 0.19mm ID and 0.8K in 0.51mm ID, respectively. Such temperature variation may be due to the bubble generation inside the tube. The wall temperature distribution is obtained from the average of the temperature history over 30 minutes.

The wall temperature distribution in the 0.19mm ID tube at $\dot{m}$ =145kg/m²s is shown in Fig. 4. When q''=5.46 kW/m², the wall temperature measured is in accordance with the saturated temperature between x=0.04m and 0.20m. Thus, saturated boiling should occur in this region. On the other hand, the wall temperature for the smaller heat flux (q''=2.61 kW/m²) monotonically increases with the axial distance, and reaches 110°C at x =0.27 m. This is due to the superheat liquid phenomena [7], which is observed in very small diameter tubes. Figure 5 shows the temperature distribution in the 0.51mm ID tube. When q''=2.82kW/m², the wall temperature increases with x and reduces a maximum value of 45°C at x=0.15 m. Since the temperature drops to the saturated temperature further downstream, the superheat liquid phase should exist between x=0.05 and 0.15 m. On the other hand, normal saturated boiling is observed for a higher heat flux of q''=12.6 kW/m².

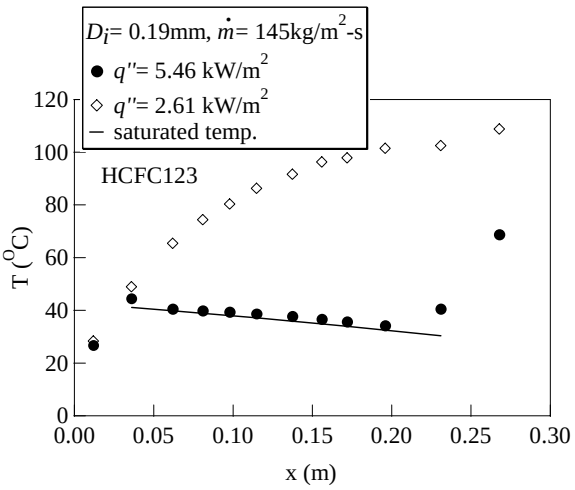

Fig. 4 Axial wall temperature distribution in 0.19mm ID.

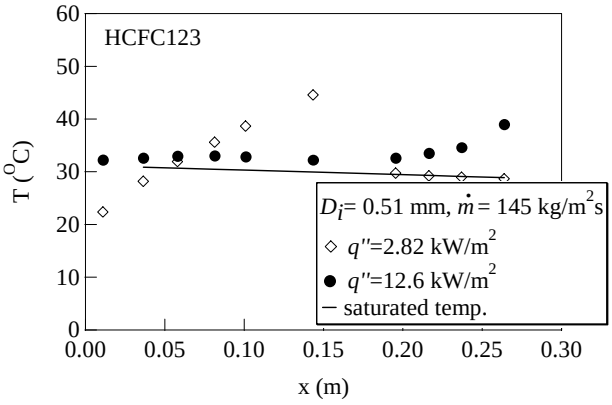

Fig. 5 Axial wall temperature distribution in 0.51mm ID.

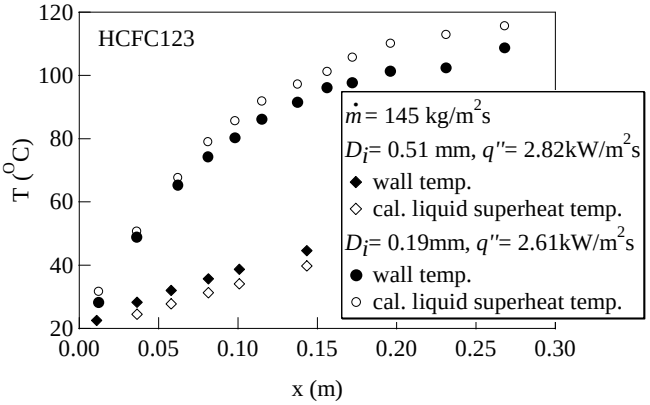

Fig. 6 Axial wall temperature distribution under superheat liquid condition in 0.51 and 0.19 mm ID.

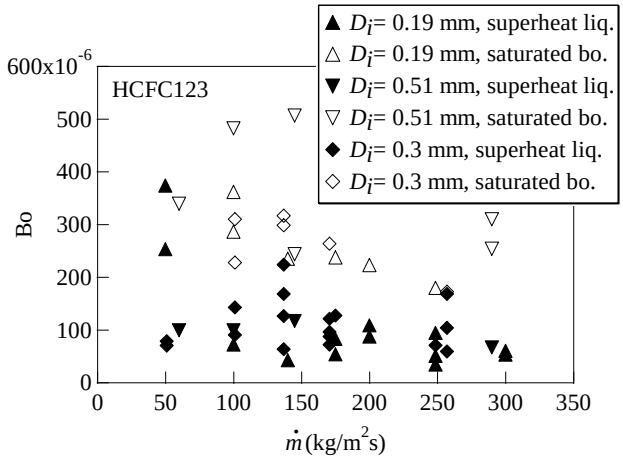

Fig. 7 Onset of liquid superheat for different inner diameters.

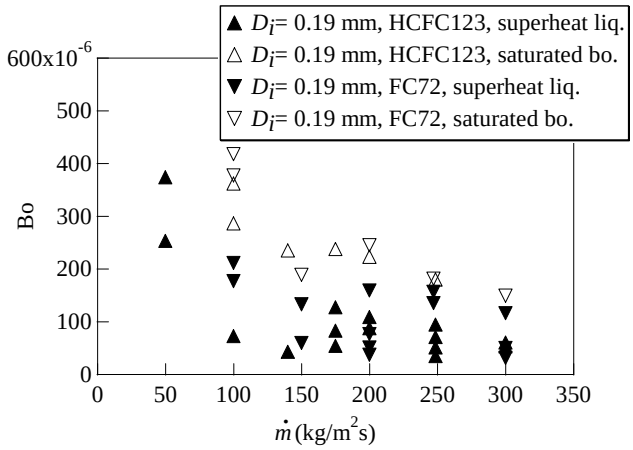

Fig. 8 Onset of liquid superheat for different refrigerants.

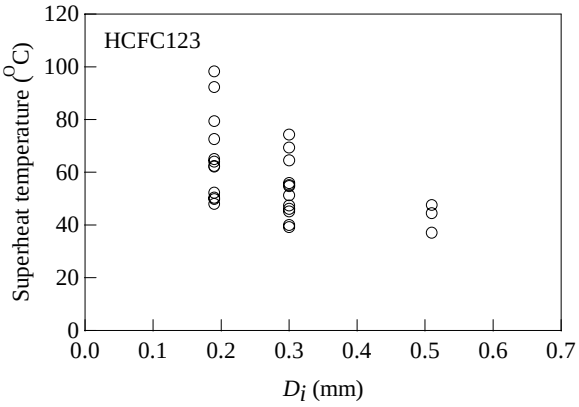

Fig. 9 Superheat temperature versus inner diameter.

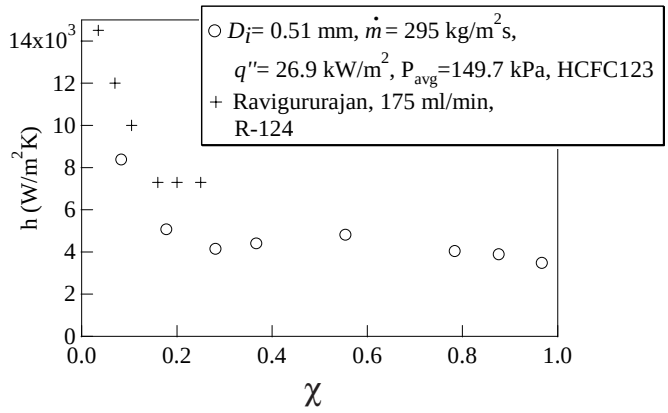

Fig. 10 Typical heat transfer coefficient distributions in microtube/ microchannels.

Figure 6 shows the wall temperature distribution under the superheat conditions in Figs. 4 and 5. Open symbols represent the fluid temperature estimated using the heat flux and heat capacity of the saturated liquid. For the 0.51mm ID tube, the temperature difference ΔT ($=T_{win}$-T_{ref}) between the wall and the fluid is constant, and the Nusselt number defined with ΔT is in good agreement with its laminar flow value of 4.364. On the other hand, the fluid temperature is overestimated for the 0.19mm ID tube, and ΔT becomes negative. The reason is unclear at this moment, but it may due to the unknown density and heat capacity of the superheated liquid.

Although it is not shown here, the pressure drop of the superheat condition is in good agreement with the estimates based on the laminar single-phase flow assumption.

4.2 Onset of superheat phenomena

Figure 7 shows the condition map for the onset of superheat phenomena as a function of boiling number and mass flux for three inner diameters of microtubes. The onset of the superheat is limited to a region of low Bo and low mass flux and seems to be independent of the tube inner diameter. In Fig. 8, the region is plotted for two different refrigerants of FC72 and HCFC123. The superheat region is almost the same with those in Fig. 7 and also independent of refrigerants.

Figure 9 shows the superheat temperature for different tube diameters and various heat and mass fluxes. Although the superheat temperature varies in a wide range, its maximum value is 100^{O}C and 45^{O}C for 0.19mm and 0.51 mm ID tubes, respectively. Thus, the maximum superheat temperature is decreased with increasing the tube diameter as reported by Brereton et al. [7].

4.3 Heat transfer coefficients

The heat transfer coefficient without superheat is investigated. Typical distributions of the heat transfer coefficient and the vapor quality in microtubes/microchannels are shown in Fig. 10. The heat transfer coefficient decreases from 8000 W/m^{2}K to 4000 W/m^{2}K with increasing the vapor quality until it reaches 0.3, then remains constant at 4000 W/m^{2}K until the vapor quality reaches 1. Such heat transfer coefficient distributions are completely different from those in small or traditional-size tubes where the heat transfer coefficient increases with increasing the vapor quality because of the convective boiling effect [8].

Ravigururajan [6], however, also found similar results in his experiments of microchannel evporators with 425μm hydraulic diameter with similar mass fluxes; one of his results is plotted in Fig. 10. The heat transfer coefficient distributions are similar. Since most of the experimental parameters (including channel shape and length, heat flux , etc.) are different except inner diameter of the channel in these two experiments, we can conclude that these unusual heat transfer coefficient distributions are due to the micro-scale geometry of the tube/channel.

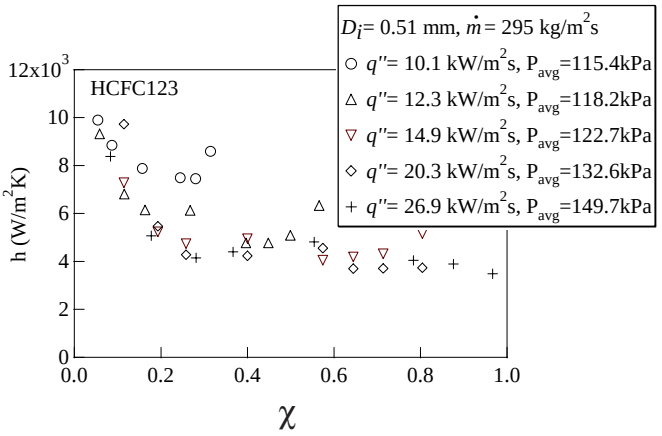

Fig. 11 Dependence of heat transfer coefficient on quality with different heat flux.

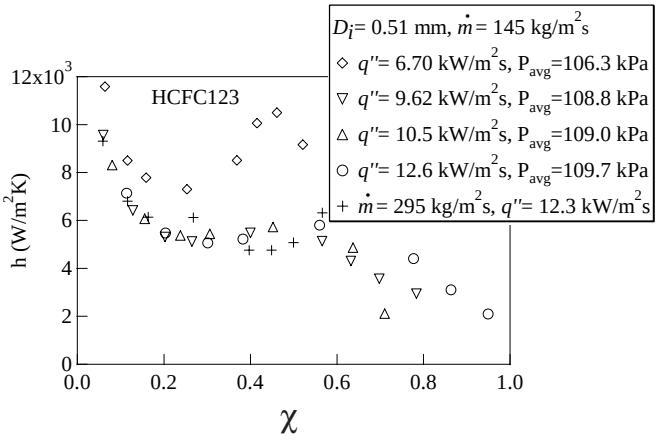

Fig. 12 Dependence of heat transfer coefficient on quality with different heat flux.

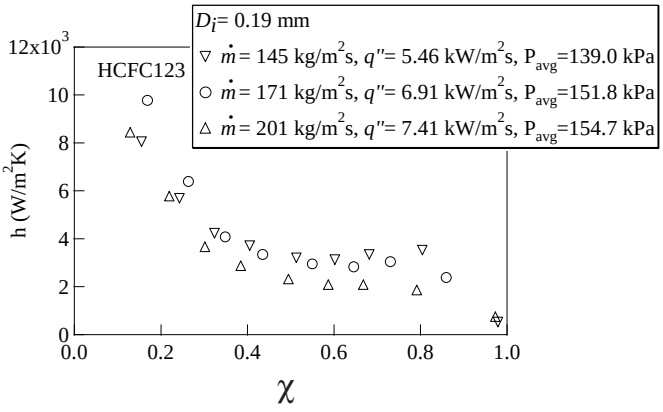

Fig. 13 Dependence of heat transfer coefficient on quality with different mass and heat flux.

The relations of heat transfer coefficient and quality under different heat , mass fluxes and average pressure in the test section are shown in Figs. 11, 12 and 13. As described above, all the heat transfer coefficients decrease with increasing the vapor quality until the vapor quality reaches about 0.3. The heat transfer coefficient also decreases with increasing the heat flux, but it remains independent of the heat flux when the heat flux is larger than 10kW/m^2. This phenomenon is different from that in traditional or small-size tubes, in which the heat transfer coefficient increases

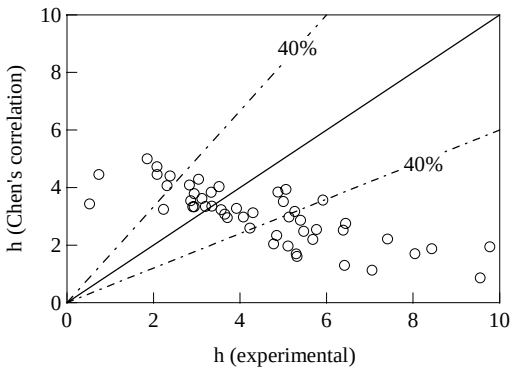

Fig. 14 Comparison of measured heat transfer coefficient with Chen's empirical correlation.

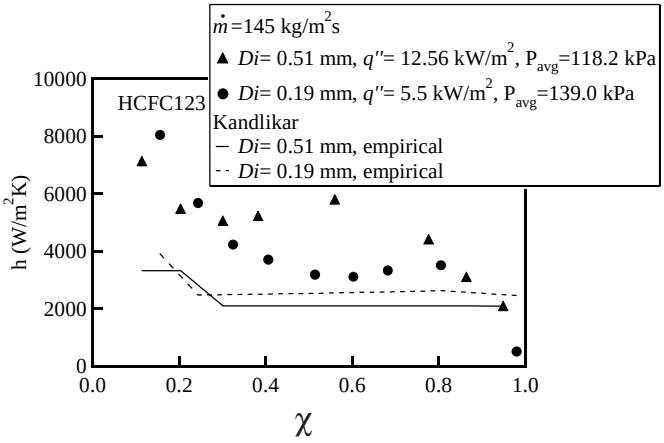

Fig. 15 Heat transfer coefficients on tube diameter and their comparison with the nucleate term of Kandlikar's empirical correlation.

with increasing the heat flux, but again coincides with the experimental results by Ravigururajan [6].

The measured heat transfer coefficients have been compared with the existing empirical correlations designed for traditional or small-size tubes. As a result, it is found that most empirical correlations underpredict/overpredict our experimental data (more than an order), except the Chen's correlation [9], which can only roughly predict our results as shown in Fig. 14. More than 50% of the experimental data falls within the +40% range of the empirical prediction.

It is also found that the nucleate boiling term of some empirical correlations can roughly predict our results, e.g., Kandlikar's empirical correlation [10] and Liu and Winterton's correlation [11]. As an example, the comparison of the experimental results and the nucleate boiling term of Kandlikar's correlation is shown in Fig. 15. From this comparison, we can learn that the nucleate boiling term of the empirical equation can predict the experimental results more precisely in 0.19mm ID than in 0.51mm ID. From this fact, we can conclude that when the inner diameter of the microtube decreases, the effect of the convective boiling decreases and the nucleate boiling effect becomes dominant gradually.

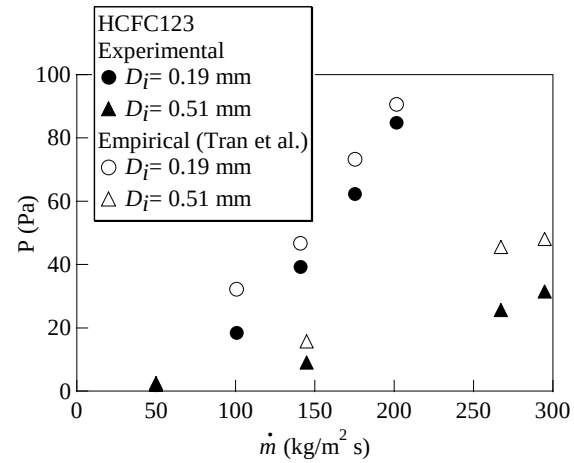

Fig. 16 Pressure loss versus mass flux when c=1.

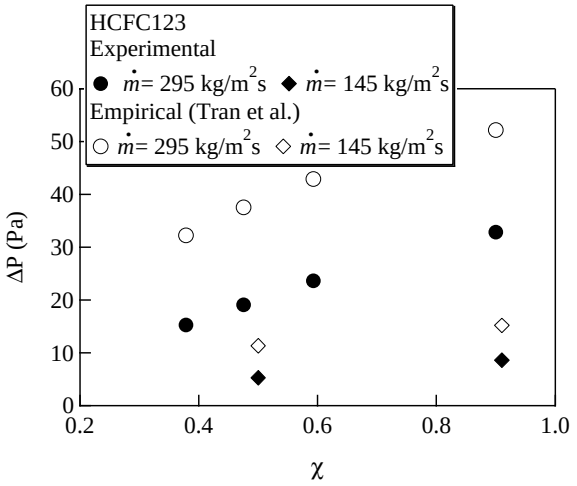

Fig. 17 Pressure loss versus vapor quality in 0.51mm ID.

4.4 Pressure losses

Figure 16 shows the relationship between the pressure loss and the mass flux when the exit quality is maintained at 1. It is found that the larger mass flux causes larger pressure loss. Figure 17 shows the relationship between the exit vapor quality and the pressure loss in the 0.51mm ID tube. Different from the heat transfer coefficient, the pressure loss distribution is similar to that in traditional or small size tubes [12]. We also compared the measured pressure loss to the empirical functions designed for small tubes of 2.46 and 2.92mm ID [12]. It is found that the trend of our experimental results is similar to these empirical correlations, but the value is much lower. The difference between them becomes larger when the inner diameter and the mass flux becomes larger.

5. Conclusions

1. High degree superheat phenomena, which had seldom been discovered in convective boiling of the traditional or small-size tubes, were observed in this experiment. This superheat phenomena deteriorate the heat transfer coefficient of microtubes under the low heat and mass flux conditions.
2. The superheat condition is given as a region map, which seems to be independent of the inner diameter and different kinds of freon-type fluids, while the maximum superheat temperature decreases with increasing the inner diameter of the microtube.
3. The heat transfer coefficient and pressure loss characteristics without superheat were investigated. The former differs from those in traditional or small-size tubes, but the latter exihibits the similar trend. The local heat transfer coefficient first decreases and then becomes almost constant with increasing the vapor quality. This constant remains almost the same when the heat flux increases beyond some threshold value.
4. Most of the current empirical correlations can not predict our results except the Chen's correlation. Some of the nucleate boiling terms of the current empirical correlations can very roughly predict our results. This means that the nucleate boiling effect dominates in heat transfer in microtubes. The empirical pressure loss correlations, however, have the same trend as the experimental results, but give somewhat higher values.

Acknowledgement

The present work is supported through the Grant-in-Aid for Scientific Research (No. 13305015) by the Ministry of Education, Culture, Sports, Science and Technology.

References

1. Mehendale, S. S., Jacobi, A. M. and Shah, R. K., Fluid flow and heat transfer at micro- and meso-scales with application to heat exchanger design, *Appl. Mech. Rev.*, Vol. 53, no.7, pp. 175-193, 2000. **2.** Kandlikar, S.G., , Fundamental Issues Related To Flow Boiling In Minichannels And Microchannels, *Experimental Thermal and Fluid Science*, Vol. 26, No.2-4 pp 389-407, 2002 **3.** Yen, T. H., Nasu, H., Suzuki, Y. and Kasagi, N., Forced Convective Boiling Heat Transfer in a Micro Tube, *Proc. Thermal Engineering Conf.*, JSME, Okayama, pp. 625-626, 2001. **4.** Paitoonsurikarn, S., Kasagi, N. and Suzuki, Y., Optimal Design of Micro Bare-tube Heat Exchanger, *Proc. Symp. Energy Engineering in the 21st Century*, Hong Kong, Vol. 3, pp. 972-979, 2000. **5.** Wambsganss, M. W., France, D. M., Jendrzejczyk, J. A. and Tran, T. N., Boiling Heat Transfer in a Horizontal Small-Diameter Tube, *J. Heat Transfer*, Vol. 115, pp. 963-972, 1993. **6.** Ravigururajan, T. S., Impact of Channel Geometry on Two-Phase Flow Heat Transfer Characteristics of Refrigerants in Microchannel Heat Exchangers, *J. Heat Transfer*, Vol. 120, pp. 485-491, 1998. **7.** Brereton, G. J., Crilly, R. J., Spears, J., R., Nucleation in Small Capillary Tubes, *Chem. Phys.*, Vol. 230, pp. 253-265, 1998. **8.** Zurcher, O., Thome, J. R. and Favrat, D., Evaporation of Ammonia in a Smooth Horizontal Tube: Heat Transfer Measurements and Predictions, *J. Heat Transfer*, Vol. 121, pp. 89-101, 1999. **9.** Chen, J.C., Correlation for Boiling Heat Transfer to Saturated Fluid in Convective Flow, *I and EC Process Design and Development*, Vol. 5, pp. 322-329, 1966. **10.** Kandlikar, S. G., A General Correlation for Saturated Two-Phase Flow Boiling Heat Transfer Inside Horizontal and Vertical Tubes, *J. Heat Transfer*, Vol. 112, pp. 219-228, 1990. **11.** Liu, Z. and Winterton, R., H., S., A General Correlation for Saturated and Subcooled Flow Boiling in Tubes and Annuli, Based on a Nucleate Pool Boiling Equation, *Int. J. Heat Mass Transfer*, Vol. 34, No. 11, pp. 2759-2766, 1991. **12.** Tran, T. N. Chyu, M. -C., Wambsganss, M. W. and France, D. M., Two Phase Pressure Drop of Refrigerants During Flow Boiling in Small Channels: An Experimental Investigation and Correlation Development, *Int. J. Multiphase flow*, Vol. 26, pp. 1739-1754, 2000.